

Analysis of Ice-Shaped Surface Roughness Based on Fractal Theory

NONG Li^{1,3}, XIAN Jun², HU Zhanwei³, ZUO Chenglin³, YI Xian^{3*}

1. School of Systems Science and Engineering, Sun Yat-Sen University, Guangzhou 510000, P.R. China;

2. School of Mathematics, Sun Yat-Sen University, Guangzhou 510000, P.R. China;

3. Icing and Anti/de-icing Key Laboratory of China Aerodynamics Research and Development Center, Mianyang 621000, P.R. China

(Received 2 April 2023; revised 10 April 2023; accepted 24 April 2023)

Abstract: The shape of ice accretion on aircraft surfaces is crucial to icing wind tunnel tests. Currently, geometrical parameters of ice, such as height, angle, and location, are used to characterise the ice shape from a 2-D perspective. However, the surface roughness of ice-shape, which is crucial to aerodynamic analysis, is always ignored. In this paper, the fractal theory is used to characterise the ice roughness, and the corresponding characterisation method is explained. An aerofoil-icing test is conducted in a large icing wind tunnel to verify the feasibility and validity of the proposed method. In the test, the icing growth information of the aerofoil surface is collected using laser line scan technology. Then, the 3-D ice shape is reconstructed using the collected data. Subsequently, the 3-D ice shape is analyzed using fractal theory, where the profile curves at different positions of the ice shape are extracted. Additionally, the corresponding fractal dimension and joint roughness characterisation are calculated to summarise the linear regression equations of the fractal dimension. Then, the data points from profile curves are extracted to simulate the fractal interpolation functions of the ice. Correlation analyses show that ice accretion on the aircraft surface exhibits fractal features, and the fractal dimension is proportional to the joint roughness characterisation, which can be used as the assessment parameter of surface roughness of ice. Consequently, the fractal interpolation simulation of the ice-shape curves represent an excellent approximation of the ice accretion on aircraft surfaces. The fractal characterisation of rough surfaces provides a new approach for scientifically quantifying 3-D ice features.

Key words: roughness; fractal theory; box-counting dimension; multiple regression analysis; characterisation

CLC number: V321.2

Document code: A

Article ID: 1005-1120(2023)02-0169-10

0 Introduction

Aircraft icing is a common phenomenon that can cause dangers during flights. Consequently, numerous studies have focused on icing predictions, post-icing aerodynamic characteristics, and aircraft icing-safety protection. In particular, analysis of ice formation mechanisms, ice types, and the ice evolution law on aircraft surfaces is a fundamental research field. Due to the influence of atmospheric conditions and flight parameters, ice accretion on aerofoils occurs in various shapes and sizes, with complex and irregular structures. Consequently, quantitatively evaluating the structural characteris-

tics of ice can be challenging. Some studies focus on quantitatively describing the 3-D ice shape. Currently, 2-D quantification methods are used. However, these methods rely on a single parameter, such as the angle and height of the ice horn, making the characteristics of the ice shapes difficult to be fully described.

Moreover, other studies have shown that roughness greatly affects the aerodynamics of the aircraft, the convective heat transfer of the surface, and the final form of the ice after icing^[1-3]. Nevertheless, when studying the effect of ice shape fidelity on aerodynamic performance^[4-5], smooth simula-

*Corresponding author, E-mail address: yixian@cardc.cn.

How to cite this article: NONG Li, XIAN Jun, HU Zhanwei, et al. Analysis of ice-shaped surface roughness based on fractal theory[J]. Transactions of Nanjing University of Aeronautics and Astronautics, 2023, 40(2):169-178.

<http://dx.doi.org/10.16356/j.1005-1120.2023.02.006>

tions can adequately represent the ice accretion by neglecting the roughness of the ice surface. Therefore, establishing a systematic description of the surface roughness of complex ice shapes for aircraft icing research is required.

Since the 1990s, the effect of ice roughness has been extensively studied by experimental and numerical methods. Some studies have documented the ice growth processes using high-speed cameras. The features are manually extracted to obtain the roughness data from the photographic images^[6-9]. According to the records of early wind tunnel tests, spectral analysis can be used to calculate roughness parameters, and the results can be used for subsequent research^[10-11].

The NASA Lewis Center developed the concept of effective roughness of icing surfaces^[12], which represents the uniform distribution of equivalent particle microelements on the ice surface. Shin et al.^[13-14] proposed an empirical formula for surface equivalent particle roughness with respect to liquid water content, temperature, mean droplet diameter, chord length, and other factors. However, few test results are available and even these could be biased because of subjective factors of the researchers, making previous results inadequate. In China, little research has been conducted in this field, and most focused on the relationship between roughness and convective heat transfer, assuming the roughness parameters without systematic research^[15-18]. Most of the ice-shaped surfaces simulated by these assumed parameters have been uniformly structured with undulating morphologies, while ice surfaces are disordered and uneven. Consequently, the simulated results have differed substantially from the experiments.

The fractal theory was proposed in the 1970s^[19], drawing much attention in the fields of economics, material engineering, chemistry, and various other disciplines^[20]. As an inimitable branch of mathematics, fractals provide a theoretical foundation to analyse irregular objectives in natural and human society. It should be noted that surface roughness measurements and characterisation have

long been research topics in tribological simulations^[21-22], and their research methods have certain implications to the scientific characterisation of ice-shaped surface roughness.

Consequently, this study uses the fractal theory to analyze the characteristics of ice surfaces. Firstly, a laser scanning measurement system is used to scan the ice accretion in an ice wind tunnel, process the scanned data, and reconstruct the 3-D digital ice form. Secondly, the ice growth process is examined to verify whether the ice has a fractal structure. Subsequently, the fractal dimension and joint roughness coefficients of the surface profile curve derived from the digital model are calculated, and the correlation between the fractal dimension and joint roughness coefficients is explored. Finally, the fractal dimension of ice used to construct the fractal interpolation curves is determined to reconstruct the ice-shaped surfaces.

1 Fractal Theory Analysis for Ice Joint Roughness

1.1 Fractal definition

A fractal is defined to be a set for which the Hausdorff dimension strictly exceeds the topological dimension. However, this definition excludes some sets with evident fractal characteristics. Thus, the definition is improved and a fractal is defined to be a set F holding the following properties^[19]:

(1) F has a fine structure, i.e., detailed at arbitrarily small scales.

(2) F has many irregularities that can be difficult to describe by traditional geometrical language, both globally and locally.

(3) F has some forms of self-similarity, approximate or statistical.

(4) Usually, the fractal dimension of F is greater than its topological dimension.

(5) In most cases, F can be defined in a simple way, for example, recursively.

1.2 Fractal dimension

The fractal dimension is a crucial feature parameter of fractals, usually a non-integer. In particu-

lar, the measured relationship between a fractal and the fractal dimension must obey a power law, i.e., as $\delta \rightarrow 0$, for constant c and s , then

$$M_\delta(F) \sim c\delta^{-s} \quad (1)$$

where s is the dimension of the fractal set F , and c the dimensional length of the set. If we take the logarithm of both sides of Eq.(1), then

$$\lg M_\delta(F) \sim \lg c - s \lg \delta \quad (2)$$

Note that $\lg M_\delta(F) - (\lg c - s \lg \delta) \rightarrow 0$ as $\delta \rightarrow 0$

$$s = \lim_{\delta \rightarrow 0} \frac{\lg M_\delta(F)}{-\lg \delta} \quad (3)$$

When δ is in a suitable range, the value of s can be obtained by estimating the slope of the function expressed in Eq.(2), i.e., $\lg M_\delta(F)$ and $\log \delta$.

Various methods can be used to calculate the fractal dimension. In particular, the box-counting method is simple, easy to implement and offers good suitability. It is one of the most widely used methods to calculate the fractal dimension. It uses a series of boxes or lattices whose lengths define δ that covers the fractal set. The different sizes of lattices intersecting the fractal set, denoted as $M_\delta(F)$, can then be counted. When the lattice length $\delta \rightarrow 0$, the logarithmic rate of increase in the number of covered lattices is the box-counting dimension.

1.3 Characterisation of fractal dimension of ice-shaped roughness

The first step to determine the ice surface roughness is to measure the ice shapes in an icing wind tunnel. Subsequently, an image processing method can be used to calculate the box-counting dimension of the ice profile at the cross-sections of ice accretion. The detailed process is shown in Fig.1.

The steps can be summarised as follows:

(1) Create 2-D ice profile prints of the cross-sections of ice accretion, with pixels of $N \times N$, $N = 2^k$, $k \in \mathbb{N}^+$. Then, convert the image into a binary image, and develop a 0 and 1 pixel matrix.

(2) Divide the pixel matrix into two disjoint blocks, and each block is a $\omega \times \omega$ matrix, where $\omega = 2^i$ ($i = 0, 1, 2, \dots, k$). Then, record the number of blocks containing element "1", denote them as

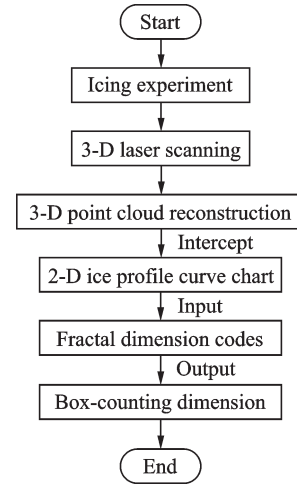


Fig.1 Algorithm for determining ice-shaped surface roughness

$M_\omega(F)$, and repeat the procedure for all blocks to obtain a sequence of $(\omega, M_\omega(F))$.

(3) Obtain a diagram by fitting the data $(-\lg \omega, \lg M_\omega(F))$ using the least square method. Calculate the slope of the fitting line, and the box-counting dimension will be obtained when the slope takes a negative value.

2 Measurement of 3-D Ice Shapes in Icing Wind Tunnels

2.1 Testing equipment and method

Icing experiments for a straight wing were performed in a $3 \text{ m} \times 2 \text{ m}$ icing wind tunnel in China Aerodynamics Research and Development Centre. The span and chord of the wing were 1.98 m and 2.2 m, respectively. The main material was aluminium alloy. The operating condition were as follows: $H = 3 \text{ km}$, $V = 50 \text{ m/s}$, $T_s = -22.5 \text{ }^\circ\text{C}$, $\alpha = 3.5^\circ$, $MVD = 20.0 \text{ } \mu\text{m}$, and $LWC = 0.8 \text{ g/m}^3$.

During the experiments, a visible laser line scanning system was used to recover the 3-D shape development of the continuous growth of ice accretion on the model. The system included a high-speed camera, a laser, and a high-precision rotating platform. The camera imaging resolution was $4096 \text{ pixel} \times 3000 \text{ pixel}$, and the maximum frame rate under full frame was 68 frame/s. The diameter of the high-precision rotating platform was 102 mm with a rotational angle range of 360° , at a resolution

of 0.01° . Moreover, the fastest speed was approximately $20^\circ/\text{s}$ with positioning accuracy repeatability of $\leq \pm 0.005^\circ$. The laser output wavelength was approximately 635 nm, and the minimum line width was approximately 1 mm. The output power could be adjusted from 0 to 120 mW.

When measuring the iced surface, the laser produced a laser sheet that was projected onto a reflector, and the reflection was re-projected onto the iced surface of the model. The reflector was then rotated using a high-precision rotary table, controlling the laser sheet scan of the iced surface. This system did not require spatial movement during measurement, so it could be installed on any side frame of the icing wind tunnel test section. The test site is shown in Fig.2.

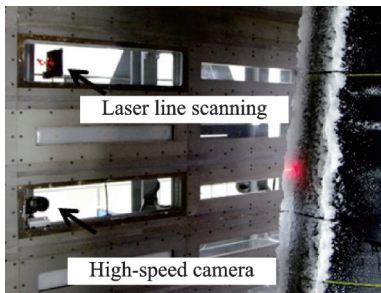


Fig.2 Equipment and test site

2.2 Testing results

During the experiment, a single scan was performed at four different time, i.e., 5, 10, 15, and 20 min. The span of the scanned model was 30 mm, and the ice growth on the wing was measured. The Meshmixer software application was used to reconstruct the digital ice surfaces using 3-D points clouds, as shown in Fig.3.

Post-processing was performed to intercept the 2-D ice profile at cross-sections of the ice accretion. For example, the profile at $X = 40$ mm and $t = 10$ min is shown in Fig.4.

2.3 Fractal characteristics of growth ice

Fig.5 shows an image from a field measurement. At early stages of the icing process, super cooled droplets define the leading edge and water-film development. Owing to instability, the surface of the film begins to exhibit roughness^[23-24]. As the

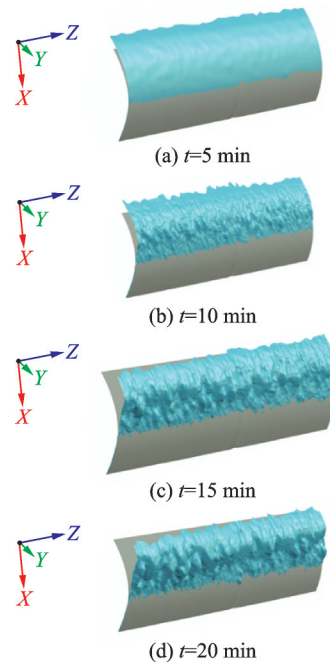


Fig.3 Single scan performed at four different time

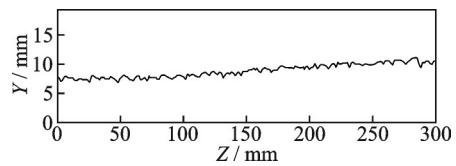


Fig.4 Profile curves ($X = 40$ mm, $t = 10$ min)

unfrozen water flows back along the chord, it breaks up into individual rivulets. Thus, the roughness elements on the water film can be observed as nucleation points.

The rough layer thickens over time, which makes it difficult for the droplets to be collected on the leeward sides. Thus, the icing volume of wake regions decreases. Moreover, the increase in roughness is accompanied with a decrease in the thickness of the boundary layer and the roughness elements interacting with flows, enhancing the convective heat transfer.

At a later growth stage ($t = 15\text{--}20$ min), the distribution of roughness elements on the wing remains practically constant. Moreover, the ice is superimposed in the previous locations, and the growth rate of roughness elements is becoming appropriate.

It should be noted that the actual objective hardly satisfies the first property of fractals, and is usually restricted to a particular scale. The character-

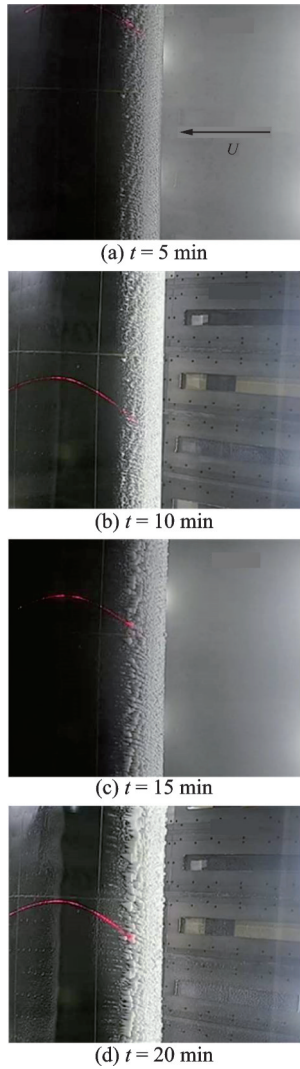
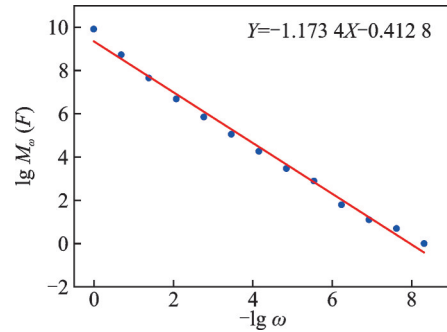


Fig.5 Leading edge ice time sequence

istic scale for this paper is the millimetre scale. For the ice macroscopic roughness characteristics, the ice crystals at the millimetre scale are small structures, so the first property is satisfied. Visually, ice presents a complex and disordered form, both globally and locally. By magnifying the ice profile, the observed icing regions are uncompleted, with several fine peaks. Thus, ice formation has self-similarity, and its growth process is scale-independent. At the mid-growth stage, the constant impact of droplets increases the height of the elements roughness, forming the final ice shape. The growth ice is similar in structure to the final ice shape, which is an iterative process. Subsequently, the fractal dimension of the 2-D ice profile can be calculated using the box-counting dimension method, as shown in Fig.6 ($X = 40$ mm and $t = 10$ min). Its box-counting di-

mension is 1.173 4, which is greater than its topological dimension. Thus, each fractal property can be verified, demonstrating that the ice on the wing can be considered as a fractal set.

Fig.6 Box-counting dimension of profile curves ($X = 40$ mm, $t = 10$ min)

3 Analysis of Ice Roughness and Fractal Dimension

Fig.7 shows the 2-D ice profile at the cross-sections of the ice accretion. Figs.7(b—e) show the interceptions at different locations ($X_1 = 10$ mm, $X_2 = 20$ mm, $X_3 = 30$ mm, and $X_4 = 40$ mm) and different time ($t_1 = 5$ min, $t_2 = 10$ min, $t_3 = 15$ min, and $t_4 = 20$ min).

3.1 Ice roughness and fractal dimension calculation

In actual engineering applications, the arithmetical mean deviation of the profile (R_a), the ten-point height of irregularities (R_z), and the maximum height of the profile (R_y), are the primary evaluation parameters for surface roughness^[25]. In particular, R_a is the absolute arithmetic mean of the contour deviated distance $|y_i|$ within a sample range of the part surface, which can be determined as

$$R_a = \frac{1}{n} \sum_{i=1}^n |y_i| \quad (4)$$

R_z is defined as the sum of the average of five contour peak heights and the average of five contour bottom depths. It can be determined as

$$R_z = \frac{1}{5} \left(\sum_{i=1}^5 y_{pi} + \sum_{i=1}^5 y_{vi} \right) \quad (5)$$

R_y is defined as the distance within the sample length from the peak line (y_{pmax}) to the bottom line

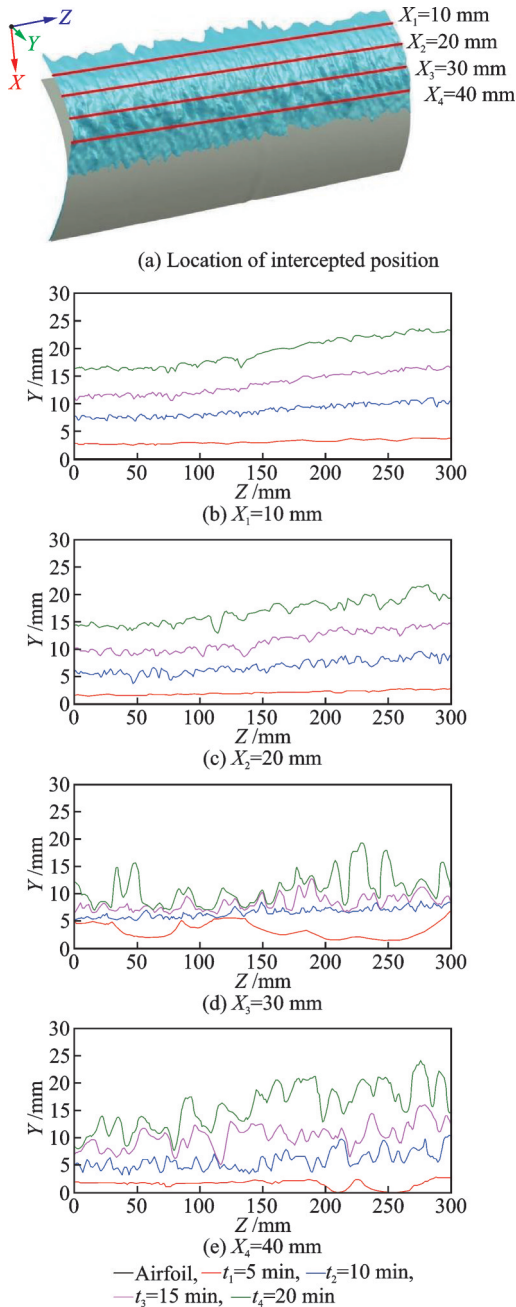


Fig.7 Profile curves at different chord wise positions

(y_{vmax}). It can be determined as

$$R_y = y_{pmax} + y_{vmax} \quad (6)$$

The results of roughness parameters of profile curves are summarized in Table 1. In Table 1, D is the box-counting dimension.

3.2 Correlation analysis

The relationship between the roughness and the fractal dimension was studied. In particular, a correlation analysis was performed to determine if the two variables were correlated^[26]. Pearson correlation is a typical measure of the degree of correla-

Table 1 Calculated results of roughness parameters of profile curves

Location/ mm	Time/ min	R_a	R_z	R_y	D
10	5	0.365 2	1.2079	1.319 8	1.131 5
	10	1.015 2	3.929 2	4.188 5	1.169 4
	15	1.801 2	6.107 2	6.281 3	1.157 6
	20	2.586 3	7.744 9	7.977 2	1.157 4
20	5	0.350 7	1.265 1	1.376	1.127 4
	10	1.054 8	5.262 7	5.847 5	1.171 4
	15	1.710 1	5.949 3	6.161 9	1.171 7
	20	2.026 7	8.363 6	8.831 2	1.177 5
30	5	0.475 1	2.645 4	2.838 4	1.140 5
	10	1.349 9	6.726 3	7.242 3	1.235 5
	15	1.758 1	10.159 8	10.965 1	1.233 2
	20	3.302 4	15.599 5	16.381 2	1.259 5
40	5	1.209 6	4.327 2	5.488 9	1.143 2
	10	0.737 1	3.336 4	3.522 6	1.173 4
	15	1.146 5	6.218 2	6.409 1	1.211 2
	20	2.326 5	11.858 7	12.250 3	1.259 5

tion between two variables, and this measure ranges between -1 and 1 . A positive value implies a positive correlation, while a negative value implies a negative correlation. The Pearson correlation coefficients between R_a, R_z, R_y and the box-counting dimension D were calculated, as shown in Fig.8.

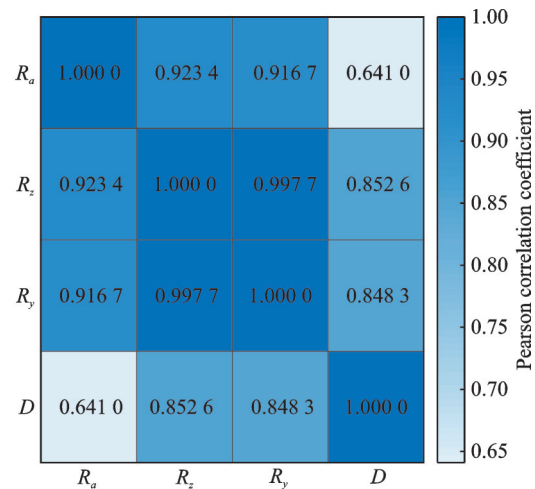


Fig.8 Pearson correlation coefficients

Fig.8 shows that all coefficients are positive. Thus, the roughness is positively correlated with the fractal dimension. The correlation coefficient between R_a and D is between 0.6 and 0.8 , implying a strong correlation. The correlation coefficients for both R_z and R_y are greater than 0.8 , implying a very

strong correlation. Consequently, fractal analyses can be further evaluated.

3.3 Multiple regression analysis

If the fractal dimension associated with a single roughness coefficient is used to express the rough surface, there could be a problem that the fractal dimension may not correspond to the roughness. For instance, the roughness parameters of profile $X = 40$ mm and $t = 10$ min decrease overall, although the fractal dimension increases. Consequently, the problem requires a multi-variable coupling analysis.

Regression analysis is a set of statistical processes for estimating the relationship between a dependent variable and one or more independent variables. Considering R_a , R_z , and R_y as independent variables and the box-counting dimension as a dependent factor, a multiple regression analysis using two regression models can be performed^[27-28].

3.3.1 Regress regression method

Regress regression methods are typically used in regression analysis. These methods can remove abnormal samples during the analysis to improve the fit of the regression equation. In this paper, multiple regression analysis was performed, and the residuals for each sample are shown in Fig.9.

The vertical lines in Fig.9 indicate the confidence intervals of the residuals for each sample, which are close and involve the zero value. The tenth sample does not contain zero values and is an outlier sample, which is removed from subsequent analyses. Thus, only normal samples are consid-

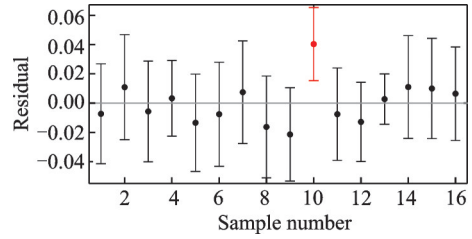


Fig.9 Residual results from regression analysis

ered, and the regression formula of the box-counting dimension is expressed as

$$D = -0.0498 \times R_a + 0.041 \times R_z - 0.0207 \times R_y + 1.1324 \quad (7)$$

$$R^2 = 0.9394, F = 56.8644, P = 5.5176E - 07$$

where R^2 measures the goodness of fit and takes values between 0 and 1. The closer to 1 this value is, the better the fit. In this case, $R^2 = 0.9394$ implies that the fitted equation has a high fitting degree. Additionally, F is a parameter that allows evaluating whether the sample is appropriate for analysis, i.e., it can verify eligibility. The probability P corresponding to F represents the confidence level of the result. The smaller the value, the higher the confidence in the result. A value of $P = 5.5176E - 07$ implies a significance level of $\alpha = 0.05$.

3.3.2 Stepwise regression method

Stepwise regression is a variable selection regression analysis method to screen out insignificant samples and reserve variables that greatly affect the outcome of the fitted equation. This method establishes the optimal regression formula with a minimum of variables, as shown in Fig.10. In Fig.10,

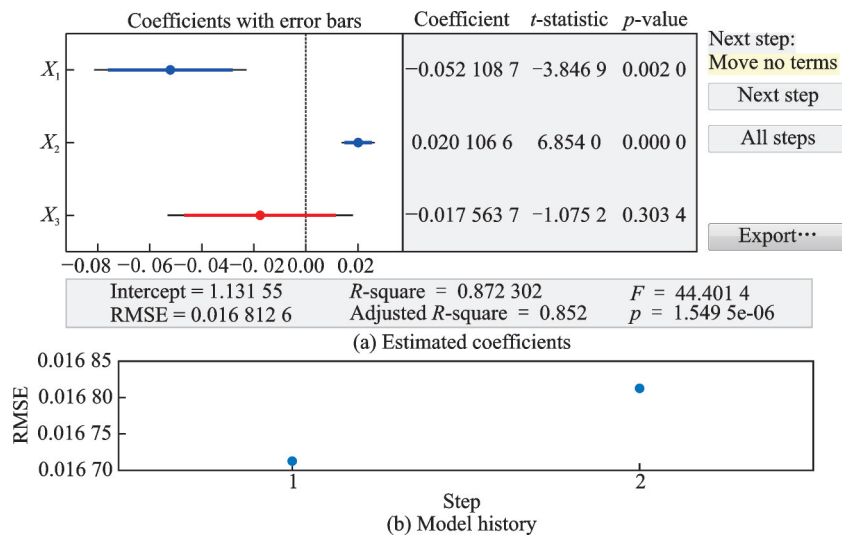


Fig.10 Stepwise regression analysis

the variables X_1 , X_2 , and X_3 in the diagram correspond to R_a , R_z , and R_y , respectively. The red text and line indicate that the variables are rejected, the blue text and line indicate that the variables are retained, i.e., only R_a and R_z are considered for fitting the fractal dimension equation

$$D = -0.0521 \times R_a + 0.02 \times R_z + 1.13155 \quad (8)$$

$$R^2 = 0.872302, F = 44.4014, P = 1.5495E - 06$$

The results clearly indicate that the fit is good, and the equation holds. The results of the fit for both models can be summarized as follows:

(1) The regression formulas for both models fit well, demonstrating that the linear relationship between the fractal dimension and the roughness parameters holds.

(2) Both models are practical and effective. In particular, the stepwise regression model screens out some variables that do not contribute significantly. Thus, this method helps to intuitively understand the variables that have a major influence. Moreover, if multiple independent variables are present, this method can improve data availability and rationality. However, removing the independent variables can cause other problems, such as Edgenuity.

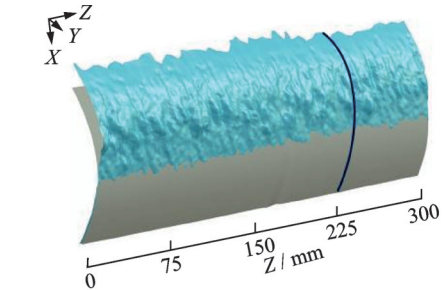
(3) Due to the small sample size collected, the applicability of the obtained equation is limited.

4 Fractal Interpolation Simulation of Ice Shape

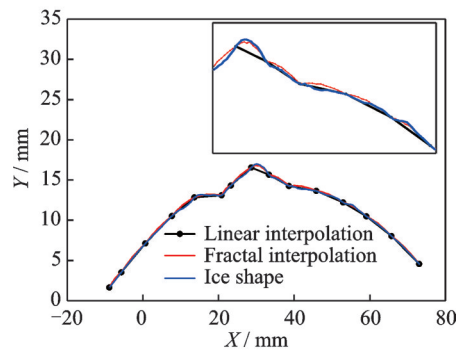
Based on the above mathematic model, once the correlation parameters for a particular ice profile have been calculated, a small volume of the original ice data can be combined with these parameters to interpolate an ice profile. Interpolated ice shapes have many applications, such as the numerical simulation of ice accretion on an aerofoil or the product cast of ice shape for wind tunnel tests, which require scaling and simplifying of the ice shape. Moreover, the interpolated ice shapes can be highly effective in generating digital ice shapes by simply using a number of original data points. Additionally, the degree of closeness and simplification from interpolation can be flexible and controllable to satisfy different engineering requirements.

In this paper, 15 points acquired from the ice

shape were used as the interpolation data for the fractal interpolation with IFS and linear interpolation^[29]. For example, the profile at $Z = 225$ mm and $t = 10$ min was considered (Fig.11).



(a) Location of the studied profile



(b) Comparison diagram

Fig.11 Fractal interpolation for ice shape

In general, the generated ice profiles by using the two interpolation methods maintain the basic contours of actual ice shapes. After enlargement, linear interpolation connects adjacent interpolation points with straight lines, covering the irregular characteristics of the data. By contrast, fractal interpolation employs the self-similarity principle to restore the rough surface of ice effectively. In this paper, fractal interpolation outperforms linear interpolation in parts with bigger horn curvature.

5 Conclusions

The fractal dimension was considered to characterise the surface roughness of ice shapes. Based on the complex ice shapes obtained from large icing wind tunnel tests, the box-counting dimension was calculated by extracting their surface profile. Subsequently, the relationship between the fractal dimension and the joint roughness coefficient was investigated, and the fractal interpolation method was used to generate digital ice shapes.

Ice formation has fractal characteristics and the fractal dimension can be used as one of the quantitative indicators to evaluate the integrity, complexity, and irregularity of ice shapes, with the integer part indicating the topological dimension of the fractal set and the fractional portion indicating the ability of the set to fill the space. The roughness quantitative evaluation method contains real information regarding the ice shape. The combined fractal dimension describes the surface structure of ice and fully reflects the ice morphology. Fractal interpolation can simulate the ice surface and display more realistic results than traditional interpolation methods.

References

- [1] HUANG Ranran, LI Dong, LIU Teng, et al. The effect of ice accretion roughness on airfoil stall characteristics[J]. *Acta Aerodynamica Sinica*, 2021, 39(1): 59-65.(in Chinese)
- [2] HUO Xiheng, CHANG Shinan. Analysis of wing surface roughness influence on icing accretion[J]. *Advances in Aeronautical Science and Engineering*, 2012, 3(2):6. (in Chinese)
- [3] WANG Qiang. Research on influence of ice accretion on airfoil surface roughness on ice shape[J]. *Aerodynamica Research & Experiment*, 2007(4):12-16. (in Chinese)
- [4] TSAO J C. Further evaluation of swept-wing icing scaling with maximum combined cross section ice shape profiles[C]//*Proceedings of 2018 Atmospheric and Space Environments Conference*. Atlanta, Georgia: [s.n.], 2018.
- [5] CAMELLO S, BRAGG M B, BROEREN A, et al. Effect of ice shape fidelity on swept-wing aerodynamic performance[C]//*Proceedings of the 9th AIAA Atmospheric and Space Environments Conference*. [S.l.]: AIAA, 2017.
- [6] ANDERSON D N, HENTSCHEL D B, RUFF G A. Measurement and correlation of ice accretion roughness[C]//*Proceedings of the 36th AIAA Aerospace Sciences Meeting and Exhibit*. [S.l.]: AIAA, 2003.
- [7] OLSEN W, WALKER E. Experimental evidence for modifying the current physical model for ice accretion on aircraft surfaces: NASA-MPD-1683[R]. [S.l.]: NASA, 1986.
- [8] HANSMAN R, REEHORST A, SIMS J. Analysis of surface roughness generation in aircraft ice accretion [C]//*Proceedings of the AIAA Materials Specialist Conference—Coating Technology for Aerospace Systems*. [S.l.]: AIAA, 1992: 298.
- [9] VARGAS M, TSAO J C. Observations on the growth of roughness elements into icing feathers [C]// *Proceedings of the AIAA Aerospace Sciences Meeting & Exhibit*. [S.l.]: AIAA, 2013.
- [10] ORR D J, BREUER K S, TORRES B E, et al. Spectral-analysis and experimental modelling of ice accretion roughness[C]//*Proceedings of the 34th Aerospace Sciences Meeting and Exhibit*. Reno, NV, USA: AIAA, 1996.
- [11] BREUER K S, TORRES B E, ORR D J, et al. Heat transfer measurements on surfaces with natural ice castings and modelled roughness[C]//*Proceedings of the 35th Aerospace Sciences Meeting and Exhibit*. Reno, NV, USA: AIAA, 1997.
- [12] RUFF G A, BERKOWITZ B M. User's manual for the NASA Lewis Ice Accretion Prediction Code (LEWICE): NASA-CR-185129[R]. [S.l.]: NASA, 1990.
- [13] SHIN J, BOND T H. Experimental and computational ice shapes and resulting drag increase for a NACA 0012 airfoil: NASA-TM-105743[R]. [S.l.]: NASA, 1992.
- [14] SHIN J. Characteristics of surface roughness associated with leading edge ice accretion[J]. *Journal of Aircraft*, 1996, 33(2): 316-321.
- [15] LI Hantao, SHU Lichun, HABASHI W G, et al. Numerical simulation of wind turbine blades aerodynamic performance based on ice roughness effects[J]. *Journal of Aircraft*, 2003, 40(6): 1212-1215.
- [16] CHANG Shinan, WANG Chao, ZHANG Yuanyuan, et al. Modelling of roughness dimension and distribution on the icing surface[J]. *Acta Aerodynamica Sinica*, 2014, 32(5): 660-667.(in Chinese)
- [17] CHENG B F, HAN Y Q, BRENTNER K S, et al. Rotor broadband noise due to surface roughness during ice accretion[C]//*Proceedings of the 54th AIAA Aerospace Sciences Meeting*. San Diego, California, USA: AIAA, 2015.
- [18] YAN L, CHAO W, CHANG S N, et al. Simulation of ice accretion based on roughness distribution[J]. *Procedia Engineering*, 2011, 17: 160-177.
- [19] MANDELBROT B B. Fractals: Form, chance and dimension[J]. *Leonardo*, 1977, 12(3): 248.
- [20] WANG Y, AZAM A, WILSON M C, et al. Generating fractal rough surfaces with the spectral representation method[J]. *Journal of Engineering Tribology*, 2021, 235(12): 2640-2653.
- [21] SUN X, MENG C, DUAN T. Fractal model of thermal contact conductance of two spherical joint surfaces considering friction coefficient [J]. *Industrial Lubrication and Tribology*, 2022(1): 74.

- [22] SUN Xianguang, MENG Chunxiao, DUAN Tiantang. A fractal model of thermal contact conductance of rough surfaces considering friction coefficient and asperity interaction[J]. Tribology, 2020, 40(5): 626-633.(in Chinese)
- [23] HUGHES M T, MCCLAIN S T, VARGAS M M, et al. Convective enhancement of icing roughness elements in stagnation region flows[C]//Proceedings of the 7th AIAA Atmospheric and Space Environments Conference. [S.l.]:AIAA, 2015.
- [24] YOON T, YEE K. Correction of local collection efficiency based on roughness element concept for glaze ice simulation[J]. Journal of Mechanics, 2020, 36(5): 607-622.
- [25] PANG G B, QI X Z, MA Q Y, et al. Surface roughness and roundness of bearing raceway machined by floating abrasive polishing and their effects on bearing's running noise[J]. Chinese Journal of Mechanical Engineering, 2014, 27(3): 543-550.
- [26] ROSS S M. Introduction to probability and statistics for engineers and scientists[M]. [S. l.]: Academic Press, 2000.
- [27] JOHNSON R A, WICHERN D W. Multivariate analysis[M]. [S.l.]: John Wiley & Sons, Inc., 2006.
- [28] HÄRDLE W K, SIMAR L. Applied multivariate statistical analysis[M]. [S.l.]: Springer, 2019.
- [29] DUTKAY D, JORGENSEN P. Iterated function systems, ruelle operators, and invariant projective measures[J]. Mathematics of Computation, 2005, 75

(256): 1931-1970.

Acknowledgements This work was supported by the National Natural Science Foundation of China (No.12132019), and the National Science and Technology Major Project (No. J2019-III-0010-0054).

Authors Ms. NONG Li received her BSc. and MSc. degrees from Guangxi Minzu University. She is a Ph.D. candidate at Sun Yat-Sen University. She focuses on ice shape parameterization and computational fluid dynamics.

Prof. YI Xian received his BSc. degree from the National University of Defense Technology and Ph.D. degree from the China Aerodynamics Research and Development Center (CARD) in 2007. In the same year, he joined CARD, where he is currently a Director Chairman of the icing and anti/De-icing Key Laboratory of China Aerodynamics Research and Development and Chairman of the committee of the Anti/De-icing branch of Chinese Society of Aeronautics and Astronautics. He focuses on icing and anti/de-icing techniques and aerodynamics.

Author contributions Ms. NONG Li proposed the major idea and wrote the manuscript. Prof. XIAN Jun advised on the manuscript. Dr. HU Zhanwei interpreted the results and advised on the manuscript. Dr. ZUO Chenglin provided model of 3D ice shape. Prof. YI Xian designed the study and conducted the analysis. All authors commented on the manuscript draft and approved the submission.

Competing interests The authors declare no competing interests.

(Production Editor: SUN Jing)

基于分形理论的翼面复杂冰形表面粗糙度分析

农 历^{1,3}, 洗 军², 胡站伟³, 左承林³, 易 贤³

(1. 中山大学系统科学与工程学院, 广州 510000, 中国; 2. 中山大学数学学院, 广州 510000, 中国;
3. 中国空气动力研究与发展中心结冰与防除冰重点实验室, 绵阳 621000, 中国)

摘要:模型表面的结冰外形是结冰风洞试验关注的核心信息, 现有研究一般采用冰角高度、冰角角度、驻点冰厚等几何参数对二维冰形进行表征, 忽略了冰形表面粗糙程度这一重要特征。针对此问题, 提出将分形理论应用于结冰冰形的粗糙度表征, 建立了基于分形理论的结冰表面粗糙度表征方法。首先在大型结冰风洞开展翼型结冰试验, 采用激光线扫描在线测量系统对结冰生长过程中不同时刻翼面结冰的表面轮廓进行测量, 获得翼面结冰的三维数值外形; 然后结合分形理论对冰形进行分析, 提取翼面不同位置冰的截面轮廓曲线, 计算截面曲线的分形维数和粗糙度表征参数, 以此归纳出分形维数的线性回归公式, 并从截面曲线中提取数据点进行分形插值模拟实测冰形。研究表明, 翼面结冰冰形粗糙表面具有分形特征; 分形维数与粗糙度表征参数呈正相关, 可作为冰形表面粗糙度的评定参数; 分形插值模拟冰形曲线, 逼近程度优异; 冰形粗糙度的分形表达法为科学量化三维冰形特征提供了新思路。

关键词:粗糙度; 分形理论; 计盒维数; 多元回归分析; 特征表征